The intestinal quorum sensing 3-oxo-C12:2 Acyl homoserine lactone limits cytokine-induced tight junction disruption

Doriane Aguanno, Garance Coquant, Barbara G Postal, Céline Osinski, Margaux Wieckowski, Daniel Stockholm, Jean-Pierre Grill, Véronique Carrière, Philippe Seksik, Sophie Thenet

TISSUE BARRIERS

Taylor & Francis
Taylor & Francis Group

Tissue Barriers

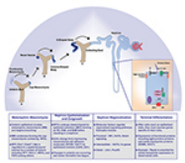

ISSN: (Print) (Online) Journal homepage: https://www.tandfonline.com/loi/ktib20

The intestinal quorum sensing 3-oxo-C12:2 Acyl homoserine lactone limits cytokine-induced tight junction disruption

Doriane Aguanno, Garance Coquant, Barbara G. Postal, Céline Osinski, Margaux Wieckowski, Daniel Stockholm, Jean-Pierre Grill, Véronique Carrière, Philippe Seksik & Sophie Thenet

To cite this article: Doriane Aguanno, Garance Coquant, Barbara G. Postal, Céline Osinski, Margaux Wieckowski, Daniel Stockholm, Jean-Pierre Grill, Véronique Carrière, Philippe Seksik & Sophie Thenet (2020) The intestinal quorum sensing 3-oxo-C12:2 Acyl homoserine lactone limits cytokine-induced tight junction disruption, Tissue Barriers, 8:4, 1832877, DOI: 10.1080/21688370.2020.1832877

To link to this article: https://doi.org/10.1080/21688370.2020.1832877

TISSUE BARRIERS
2020, VOL. 8, NO. 4, e1832877 (20 pages)
https://doi.org/10.1080/21688370.2020.1832877

Taylor & Francis
Taylor & Francis Group

RESEARCH PAPER

OPEN ACCESS Check for updates

The intestinal quorum sensing 3-oxo-C12:2 Acyl homoserine lactone limits cytokine-induced tight junction disruption

Doriane Aguanno[a,b], Garance Coquant[a], Barbara G. Postal[a,c,d], Céline Osinski[e], Margaux Wieckowski[a,b], Daniel Stockholm[a,b], Jean-Pierre Grill[a], Véronique Carrière[a], Philippe Seksik[a,f], and Sophie Thenet[a,b]

[a]Centre de Recherche Saint-Antoine, Sorbonne Université, INSERM, Paris, France; [b]EPHE, PSL University, Paris, France; [c]Université de Paris, Centre De Recherche sur l'Inflammation, INSERM UMR 1149, Paris, France; [d]Biology and Genetics of Bacterial Cell Wall Unit, Pasteur Institute, Paris, France; [e]Sorbonne Université, INSERM, Nutrition and obesities: systemic approaches, Paris, France; [f]Département De Gastroentérologie Et Nutrition, Paris, France

ABSTRACT

The intestine is home to the largest microbiota community of the human body and strictly regulates its barrier function. Tight junctions (TJ) are major actors of the intestinal barrier, which is impaired in inflammatory bowel disease (IBD), along with an unbalanced microbiota composition. With the aim to identify new actors involved in host-microbiota interplay in IBD, we studied N-acyl homoserine lactones (AHL), molecules of the bacterial *quorum sensing*, which also impact the host. We previously identified in the gut a new and prominent AHL, 3-oxo-C12:2, which is lost in IBD. We investigated how 3-oxo-C12:2 impacts the intestinal barrier function, in comparison to 3-oxo-C12, a structurally close AHL produced by the opportunistic pathogen *P. aeruginosa*. Using Caco-2/TC7 cells as a model of polarized enterocytes, we compared the effects on paracellular permeability and TJ integrity of these two AHL, separately or combined with pro-inflammatory cytokines, Interferon-γ and Tumor Necrosis Factor-α, known to disrupt the barrier function during IBD. While 3-oxo-C12 increased paracellular permeability and decreased occludin and tricellulin signal at bicellular and tricellular TJ, respectively, 3-oxo-C12:2 modified neither permeability nor TJ integrity. Whereas 3-oxo-C12 potentiated the hyperpermeability induced by cytokines, 3-oxo-C12:2 attenuated their deleterious effects on occludin and tricellulin, and maintained their interaction with their partner ZO-1. In addition, 3-oxo-C12:2 limited the cytokine-induced ubiquitination of occludin and tricellulin, suggesting that this AHL prevented their endocytosis. In conclusion, the role of 3-oxo-C12:2 in maintaining TJ integrity under inflammatory conditions identifies this new AHL as a potential beneficial actor of host–microbiota interactions in IBD.

ARTICLE HISTORY
Received 2 June 2020
Revised 21 September 2020
Accepted 23 September 2020

KEYWORDS
N-acyl homoserine lactones; N-(3-Oxododecanoyl)-L-homoserine lactone; quorum sensing; intestinal barrier; leak pathway; tight junctions; occludin; tricellulin; inflammatory bowel disease; itch

Introduction

Among the multiple actors involved in the intestinal barrier function, the intestinal epithelium plays a unique role as it physically separates the microbiota residing in the lumen from systemic tissues and limits the permeation of potential pro-inflammatory molecules from the luminal environment to the lamina propria and circulation. The intestinal epithelial barrier is achieved by the cooperation of three cell-cell junctions forming the apical junctional complex, i.e. tight junctions, adherens junctions and desmosomes, which allow epithelial cells to be tightly connected.[1] Tight junctions (TJ) are key actors in the barrier function since they seal the intercellular space and specifically control the paracellular permeability.[2] TJs are formed by a network of highly regulated multi-protein complexes, in which several classes of transmembrane proteins are connected to a cortical actomyosin belt through a variety of scaffolding and signaling proteins, including the members of *Zonula Occludens* (ZO) proteins (ZO-1, 2, and 3). This cytosolic plaque is crucial for TJ stability and dynamics.[3,4]

TJ permeability to water, ions, small or macromolecules is controlled by different families of transmembrane proteins and is modulated by numerous physiological and environmental factors. A large repertoire of claudins selectively regulates anion and cation passage, in a high capacity but highly selective "pore pathway".[5] Besides, a "leak pathway", corresponding to the permeation of

CONTACT Sophie Thenet sophie.thenet@ephe.psl.eu Centre De Recherche Saint-Antoine UMR_S, 938,Ecole Pratique Des Hautes Etudes, Paris, 75006, FRANCE

Supplemental data for this article can be accessed on the publisher's website

macromolecules, is restricted by occludin at bicellular TJs[6] and by tricellulin at tricellular TJs.[7] Contrary to the pore pathway, the passage of molecules via the leak pathway is very limited in physiological conditions.[5]

The integrity of the intestinal barrier is compromised in a variety of clinical conditions, including gastrointestinal disorders (i.e. inflammatory bowel disease, celiac disease, irritable bowel syndrome, infectious diarrheas) and extra-digestive pathologies such as type I diabetes, obesity, liver steatosis and AIDS.[8] Impairments of both pore and leak pathways have been described in these diseases and the increased passage of macromolecules such as bacterial products from the commensal microbiota is thought to be particularly harmful since it may trigger an excessive activation of the mucosal immune system.[4] Increased recruitment of leucocytes (including neutrophils, lymphocytes or macrophages) in close proximity to the epithelial lining leads to local accumulation of proinflammatory mediators such as inflammatory cytokines further exacerbating the epithelial barrier failure.[9,10] In inflammatory bowel disease (IBD), although intestinal barrier dysfunction is potentially both a cause and a consequence, several data argue for its early implication in the pathogenesis. An increased intestinal permeability was highlighted in healthy first-degree relatives of Crohn's disease (CD) patients[11,12] and was shown to predict disease relapse.[11,13] Linked with these permeability modifications, alterations of several TJ proteins, including increase in expression of the pore-forming claudin-2[14,15] and decrease in several barrier-forming claudins,[14] as well as decreased levels of JAM-A,[14,16] occludin[14,17] and tricellulin[12,15] have been reported in the intestinal mucosa of IBD patients. Most alterations were reported in active state of the disease, nonetheless several of them occurred also in the quiescent sate[12,17] or in healthy relatives,[12] highlighting intestinal barrier impairment as a possible early step in the pathogenesis of IBD[9,18] and the importance of deciphering the mechanisms involved in such defects.

Bacteria-host crosstalk plays a central role in intestinal epithelial homeostasis and is dysregulated in IBD. In recent years, our knowledge of the impact of gut-derived metabolites on the host in the context of IBD has increased considerably. Among the most studied metabolites, are short-chain fatty acids (SCFA), bile acids and tryptophan metabolites.[19] A yet poorly documented aspect of these microbiota–host interactions is the crosstalk mediated by *quorum sensing* (QS) molecules. QS is a bacterial communication network that relies on the ability of bacteria to monitor and respond to population density *via* diffusible molecules named autoinducers. Different QS systems allow bacterial populations to coordinate gene expression and behavior, and regulate a variety of physiological processes, including virulence factor production and biofilm formation.[20] Bacterial QS molecules also exert several effects on eukaryotic cells of the host, in a process named interkingdom signaling.[21]

N-Acyl homoserine lactones (AHL), which mediate auto-induction (AI)-1 type QS, are the most studied QS molecules. QS driven by AHLs has been described in many bacterial ecosystems, but its study in the gastrointestinal tract has long been restricted to pathogens.[22] In a recent study, we demonstrated for the first time the presence of 14 different AHLs in the human gut ecosystem and identified the 3-oxo-C12:2 AHL as the most conserved and abundant one in healthy subjects.[23] Importantly, 3-oxo-C12:2 AHL levels were reduced in IBD patients, more particularly during flare, and its absence was correlated with dysbiosis,[23] suggesting a beneficial role of this new molecule in the intestinal ecosystem and protective properties for intestinal mucosa.

This newly described 3-oxo-C12:2 AHL is structurally very close to the widely studied 3-oxo-C12 AHL (Figure 1). The latter is produced by *Pseudomonas aeruginosa*, an opportunistic pathogen that is the source of various infections, mostly nosocomial disease and lung infections in cystic fibrosis, and is able to cross epithelial barriers.[24] 3-oxo-C12 AHL has been shown to disturb a variety of biological processes in host cells,[25] among which perturbation of epithelial junctions. In intestinal epithelial cell lines, 3-oxo-C12 AHL induced an increased paracellular permeability to ions and macromolecules.[26,27] This was accompanied by perturbation of the localization and phosphorylation of the TJ proteins occludin, ZO-1,[27,28] tricellulin,[28] JAM-A, ZO-3,[29] together with the adherens junction proteins E-cadherin and β-catenin.[27] 3-oxo-C12:2 AHL has never been studied in this setting.

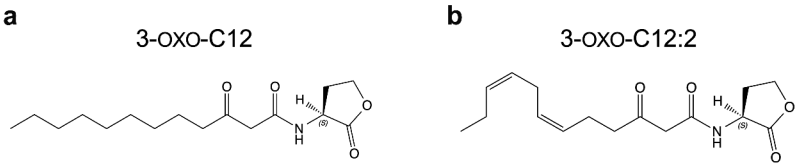

Figure 1. Chemical structure of 3-oxo-C12 and 3-oxo-C12:2 N-acyl-homoserine lactones. (a) N-(3-oxododecanoyl)-L-homoserine lactone (referred as 3-oxo-C12) is produced by *P. aeruginosa*. (b) Unsaturated 3-oxo-C12:2 homoserine lactone (referred as 3-oxo-C12:2) was identified in the human gut microbiota and was synthesized as described in.[23]

In the perspective of using QS molecules as ecological therapeutic approaches for IBD treatment, an in-depth knowledge of their effects on host is an essential step. We therefore focused on the epithelial barrier function, which is compromised during IBD. The aim of the present study was to investigate the putative beneficial role of the newly identified 3-oxo-C12:2 AHL on intestinal epithelial barrier, compared to 3-oxo-C12 AHL, thus unraveling differential effects of these two structurally close AHLs. Focusing on tight junctions as key actors of the barrier function, we addressed in particular whether the AHLs could modulate the effects of pro-inflammatory cytokines Interferon-γ (IFNγ) and Tumor Necrosis Factor-α (TNFα), known to have deleterious consequences on the intestinal epithelial barrier.[30,31] Using Caco-2/TC7 cells as a model of polarized enterocytes, we evaluated the effects of both AHLs, alone or combined with IFNγ and TNFα, on paracellular permeability and tight junction integrity. While 3-oxo-C12 AHL disrupted intercellular junctions, increased paracellular permeability and potentiated the effects of IFNγ and TNFα, we showed that 3-oxo-C12:2 AHL protected and stabilized tight junctions, through moderating the increase in occludin and tricellulin ubiquitination induced by cytokines.

Materials and methods

Cell culture and treatments

We used the Caco-2/TC7 cell line, which is a clonal population established from human colon carcinoma Caco-2 cells at late passage.[32] This cell line reproduces to a high degree most of the morphological and functional characteristics of normal human absorptive enterocytes.[32] Caco-2/TC7 cells form mature intercellular junctions, which make them a good model of intestinal epithelial barrier.[33,34] The cells were used between passages 20 and 32 (starting from cloning) and were assessed for the absence of mycoplasma contamination. Caco-2/TC7 cells were cultured in high-glucose Dulbecco's modified Eagle's medium Glutamax (Thermofisher Scientific) supplemented with 20% heat-inactivated fetal calf serum (FCS) (Eurobio Abcys, Courtaboeuf, France), 1% non-essential amino acids, penicillin (100 IU/ml), and streptomycin (100 µg/ml) in a 10% CO2/air atmosphere on semi-permeable filters (24 mm Transwell®, 3 µm pore size; Costar) for 16–18 days to reach optimal-differentiated state as described previously.[35] From confluency (7 days), cells were switched to asymmetric conditions, i.e. with medium containing 20% FCS in the basal compartment and serum-free medium in the apical compartment.

Caco-2/TC7 cells were exposed on their apical side to either N-(3-oxododecanoyl)-L-homoserine lactone (150 µM, referred as 3-oxo-C12, Sigma Aldrich) or 3-oxo-C12:2 homoserine lactone (150 µM, referred as 3-oxo-C12:2, synthesized as previously described[23]) for 48 h, in the presence of the lactonase inhibitor 2-hydroxyquinoline (100 µM, Sigma-Aldrich), in order to limit the hydrolysis of the AHL lactone ring.[23,36] Similar concentrations of 3-oxo-C12, which are in the range of doses found in biofilms,[37] were previously shown to disrupt tight junctions in the parental cell line Caco-2.[26] Both AHLs were dissolved in DMSO and then diluted in the apical medium with a final concentration of DMSO as 0.075% for all conditions including untreated control cells. When indicated Interferon-γ (IFNγ) and Tumor Necrosis Factor-α (TNFα) (50 ng/mL, R&D systems) were added in the basal compartment for 48 h. Media with treatments were daily changed. When specified, Caco-2/TC7 cells were treated with Dynasore

(Sigma-Aldrich), which was added to both apical and basal compartments (75 µM) on the last 4 hours of the experiment.

In some experiments, Caco-2/TC7 enterocytes were co-cultured with activated THP-1 monocytic cells.[38] THP-1 cells were grown at 37°C in a 5% CO2/air atmosphere in RPMI-1640 (Thermofisher Scientific) containing 10% heat-inactivated fetal calf serum and supplemented with penicillin (100 IU/ml), streptomycin (100 µg/ml) and 0.01% β-mercaptoethanol (Sigma-Aldrich). Prior to co-culture experiments, THP-1 cells were activated with LPS (10 ng/mL, Sigma-Aldrich) for 18 h. THP-1 cells were then harvested and centrifuged, and seeded (10^6 cells per well) in the basal compartment of Transwell®containing Caco-2/TC7 cells exposed on their apical side to either 3-oxo-C12 or 3-oxo-C12:2 AHL (150 µM) or DMSO (total exposure time 48 h). Co-culture was maintained for 24 h prior to permeability measurements.

Permeability measurements in Caco-2/TC7 cells

To assess paracellular permeability, FITC-labeled dextran 4 kDa (1 mg/mL; TdB Consultancy AB, Uppsala, Sweden) or FITC-sulfonic acid 0.4 kDa (0.2 mg/mL; Thermofisher Scientific) was added to the apical medium. Samples of basal medium were collected after 4 h, and fluorescence was determined with a microplate fluorometer (FLUOstar Omega; BMG Labtech). Transepithelial electrical resistance (TEER), which is inversely proportional to permeability to ions, was measured after treatment using a volt-ohm meter (Millipore, Guyancourt, France).

Lactate dehydrogenase release

The release of the cytoplasmic enzyme lactate dehydrogenase (LDH) in the apical medium was used to assess treatment cytotoxicity. LDH concentration was measured using the Cytotoxicity Detection Kit (Roche, Boulogne-Billancourt, France) according to the manufacturer's instructions. Briefly, apical media were centrifuged 10 min at 250 g to remove intact extruded cells. 50 µL of reaction mixture was added to 50 µL of media supernatant per 96-well. After 10 min at room temperature, 25 µL of stop solution was added. Absorbance at 490 nm was determined with a microplate spectrometer (FLUOstar Omega; BMG Labtech). Results are expressed as absorbance arbitrary units.

Immunofluorescence analysis of junctional proteins and image analysis

Caco-2/TC7 cells grown on 24 mm Transwell® were fixed and permeabilized with methanol (5 min, – 20°C). The following primary antibodies were used: anti-E-cadherin (rat monoclonal antibody ECCD2 M108; Takara Bio Europe; 1:1000), anti-occludin (rabbit polyclonal antibody, #71-1500; Thermofisher Scientific; 1:200), anti-tricellulin (rabbit monoclonal antibody, #700191; Thermofisher Scientific; 1:200) and anti-ZO-1 (mouse monoclonal clone 1A12, #33-9100; Thermofisher Scientific; 1:200). Alexa 488-, Alexa 546- and Alexa 647-conjugated anti-immunoglobulin G were used as secondary antibodies (1:400; Thermofisher Scientific). Nuclei were stained by 4′-6-diamidino-2-phenylindole (DAPI), and cells were examined by structured illumination microscopy using an Axio Imager 2 microscope equipped with Apotome.2, allowing optical sectioning (Zeiss, Oberkochen, Germany). Images were acquired by ZEN 2011® software (Zeiss). Quantification of fluorescent labeling was performed by measuring the staining area on thresholded images using Fiji software (https://imagej.net/Fiji/Downloads).

Proximity ligation assay (PLA) and image analysis

Following fixation and permeabilization in methanol (5 min, – 20°C), PLA was performed on cells using two primary antibodies: anti-ZO-1 or anti-ubiquitin (mouse monoclonal clone P4D1 antibody, #BML-PW0930; Enzo; 1:400) or anti-itch (mouse monoclonal clone 32/itch antibody, #611199; BD Transduction Laboratories™; 1:200) combined with either anti-occludin or anti-tricellulin. PLA PLUS and MINUS probes for mouse and rabbit and the Duolink® Orange detection kit reagents (Sigma-Aldrich) were used according to manufacturer's instructions. Nuclei were stained by DAPI, and cells were examined by structured illumination microscopy as described above. Images were acquired by ZEN 2011®

software. For Occludin/ZO-1 PLA, the high density and close proximity of spots did not allow to individualize and count PLA spots. Thus the average integrated density of a single PLA spot was calculated over 10 thresholded images per condition for each experiment and this representative value (λ) was then used to estimate the number of spots per image (estimated number of spots = integrated density of the field/λ). In order to quantify scattering of tricellulin/ZO-1 PLA spots, images were first analyzed using QuPath software[39] for the detection of spots and transferred to ImageJ.[40] The '*Tubeness*' plug-in (https://www.longair.net/edinburgh/imagej/tubeness/) was then applied to estimate the continuity of junctional networks. Data were presented as the tubeness average size. For occludin/ubiquitin, tricellulin/ubiquitin, occludin/itch or tricellulin/itch PLA assays, spots were well individualized and the number of spots per field was calculated using the '*Analyze Particles*' plug-in on thresholded images in Fiji software and was then normalized to respective fluorescence levels (based on area) of either occludin or tricellulin. All macros are available upon request.

All data were analyzed as the average from 4 to 5 random fields per biological duplicate or triplicate from three independent experiments.

Levels of mRNA junctional protein genes by (RT)-qPCR analysis

Total RNA was extracted from Caco-2/TC7 cells using TRI Reagent (Molecular Research Center, Cincinnati, OH, USA) according to the manufacturer's instructions. Reverse Transcription (RT) was performed with 1 µg RNA using a high-capacity complementary DNA (cDNA) reverse transcriptase kit (Applied Biosystem, Thermo Fisher Scientific). For claudin genes, as *CLDN4* (claudin 4) has no intron, RT was performed with 0.5 µg of previously DNAse-treated RNA (Invitrogen™ Kit TURBO DNA-free). Semi-quantitative real-time PCR was performed with the Mx3000P Stratagene system using SYBR Green (Agilent, Les Ulis, France) according to the manufacturer's procedures. Cyclophilin was used as the reference gene. After amplification, Ct were determined and relative gene expression was analyzed using the $2^{-\Delta\Delta Ct}$ method. Sequences of the oligonucleotide primers used are reported in Table 1.

Determination of protein levels by Wes™ capillary electrophoresis and ELISA

Caco-2/TC7 cells were scraped into lysis buffer (20 mM Tris-HCl, pH 7.4, 5 mM EDTA, 0.15 M NaCl, 1% Triton X-100, 0.5% sodium deoxycholate) supplemented with protease inhibitor cocktail (Complete Mini; Roche, Boulogne-Billancourt, France) and phosphatase inhibitor cocktail (PhosSTOP, Sigma-Aldrich). Protein concentrations were determined using the BC Assay (Uptima/Interchim). Wes™ analyses (capillary electrophoresis system; ProteinSimple, San Jose, CA) were performed according to the manufacturer's recommendations, and adequate protein concentrations and antibody dilutions were determined in preliminary assays in order to allow optimal quantitative conditions. The microplates were loaded with 0.8 µg/µL protein (for occludin, tricellulin and ZO-1 analysis), 0.2 µg/µL protein (for E-cadherin analysis) or 0.5 µg/µL protein (for p-MLC2 and MLC2 analysis), primary antibodies (as detailed below), and reagents provided by the manufacturer. The same primary antibodies targeting tight junction proteins were used for immunofluorescence and Wes™ analyses: anti-occludin (1:25), anti-tricellulin (1:2000) and anti-ZO-1 (1:200). For E-cadherin detection, the following antibody was used: mouse monoclonal clone 36 (#610181;

Table 1. Oligonucleotide primer sequences used for real-time PCR in this study.

TARGET GENE (protein)	Forward	Reverse
PPIB (Cyclophilin B)	5′ -GCCTTAGCTACAGGAGAGAA-3′	5′ -TTTCCTCCTGTGCCATCTC-3′
TJP1 (ZO-1)	5′ -CAGAGCCTTCTGATCATTCCA-3′	5′ -CATCTCTACTCCGGAGACTGC-3′
OCLN (occludin)	5′ -AGGAACCGAGAGCCAGGT-3′	5′ -GGATGAGCAATGCCCTTTAG-3′
MARVELD2 (tricellulin)	5′ -CAGGCTGTCCTGAGGAAGTT-3′	5′ -CCGAATGATGTGGCAATCT-3′
CLDN2 (claudin-2)	5′ -ATTGTGACAGCAGTTGGCTT-3′	5′ -CTATAGATGTCACACTGGGTGATG-3′
CLDN4 (claudin-4)	5′ -CTGTGGCCTCAGGACTCTCT-3′	5′ -CAGAGGGGATCAGTCTCCAG-3′
CLDN7 (claudin-7)	5′ -AAAATGTACGACTGCGTGCTC-3′	5′ -CACTTCATGCCCATCGTG-3′

BD Biosciences, Rungis, France, 1:1000). For Myosin Light Chain detection, the following antibodies were used: mouse monoclonal anti-MLC2 (clone 7C9, Novus, #NBP1-28871, 1:50), rabbit anti-pMLC2 (Ser19) (Cell signaling, #3671, 1:50). Data were analyzed using Compass for SW3.1 software (ProteinSimple). Occludin, tricellulin, ZO-1 levels were determined by chemiluminescence signal (AUC) and normalized to E-cadherin levels, after verification that E-cadherin levels do not differ between conditions (p = .84).

Myosin Light Chain Kinase (MLCK) concentrations were determined in total cell lysates by ELISA according to the manufacturer's instructions (CUSABIO # CSB-E09048h).

Statistical analyses

Data are displayed as means ± standard error of the mean (SEM) unless otherwise indicated. The number of independent experiments and replicates are indicated in the figure legends. Measurements of permeability (passage of FITC-dextran 4 kDa) and of cytotoxicity (lactate dehydrogenase release) were systemically carried out as internal controls of the treatment's effects for other assays, which explains the larger number of independent experiments performed for these two parameters.

Figures were created with Graphpad® Prism 6.0 (Ritme Informatique, Paris, France). Statistical analyses were performed with Graphpad® Prism 6. Statistical differences between the means of the groups were determined by either ordinary one-way ANOVA, or non-parametric Kruskal–Wallis test (when data did not pass test for normal distribution). When ordinary one-way ANOVA or Kruskal–Wallis test established statistical differences, comparisons between the following groups were performed respectively by Holm-Sidak's or Dunn's multiple-comparison post hoc tests: Control vs. all other conditions; 3-oxo-C12 vs. 3-oxo-C12:2; IFNγ+TNFα vs. IFNγ+TNFα + 3-oxo-C12; IFNγ+TNFα vs. IFNγ+TNFα + 3-oxo-C12:2; IFNγ+TNFα + 3-oxo-C12 vs. IFNγ+TNFα + 3-oxo-C12:2. $p < .05$ was considered statistically significant.

Results

Unlike 3-oxo-C12, 3-oxo-C12:2 AHL does not modify paracellular permeability

We first studied the effects of 3-oxo-C12:2 AHL compared to 3-oxo-C12 on paracellular permeability to macromolecules (assessed through the flux of the fluorescent tracer FITC-Dextran 4kDa) and to ions (assessed through the TEER, inversely proportional to the ions flux) in the enterocytic cell line Caco-2/TC7. In accordance with the literature,[26,27] 3-oxo-C12 AHL induced a 4.8-fold increase in the macromolecular FITC-Dextran 4kDa (FD4) flux (Figure 2a) and a trend toward a 10% decrease in TEER (Figure 2b) compared to untreated control cells. 3-oxo-C12:2 AHL modified neither FD4 flux (Figure 2a) nor TEER (Figure 2b). These observations support our hypothesis of a beneficial role on the epithelial barrier. We then investigated whether these AHLs could modulate an increase in paracellular permeability induced upon exposure to the two pro-inflammatory cytokines Interferon-γ and Tumor Necrosis Factor-α (thereafter referred as IFNγ +TNFα), previously shown to impair the intestinal barrier function by disrupting tight junctions.[30] IFNγ+TNFα induced a 5-fold increase in FD4 passage (Figure 2a) but had no significant effect on TEER (−5%, Figure 2b) compared to control. Strikingly, 3-oxo-C12 AHL significantly potentiated the cytokine effects on both FD4 flux (18-fold increase, Figure 2a) and TEER (30% decrease, Figure 2b). On the contrary, 3-oxo-C12:2 AHL did not modulate the cytokine-induced increase in paracellular permeability to macromolecules (Figure 2a) or to ions (Figure 2b). Similar response profiles were observed for the smaller size tracer sulfonic acid (0.4kDa, Supplementary Figure 1A). We then wanted to determine whether the AHLs modulated epithelial cell permeability in the presence of endogenous inflammatory cytokines secreted by immune cells. To this end, Caco-2/TC7 enterocytes exposed to each AHL were co-cultured with activated THP-1 monocytic cells (Figure 2c). The co-culture of Caco-2/TC7 with THP-1 cells induced a modest increase in paracellular permeability of the epithelial monolayer (1.5-fold increase, Figure 2c). While the addition of 3-oxo-C12 AHL

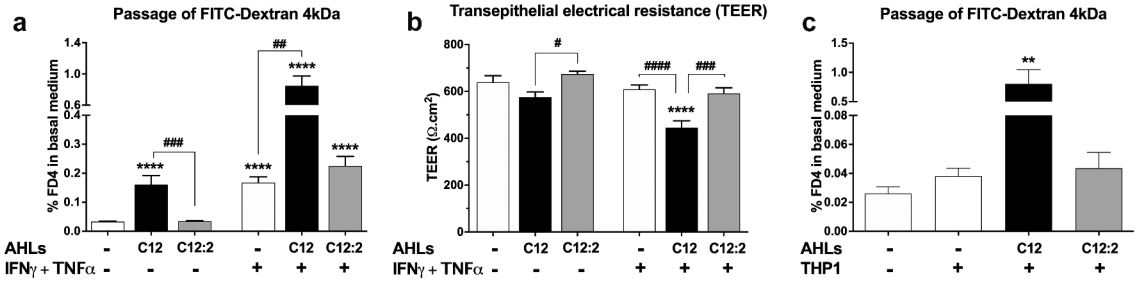

Figure 2. Distinct effects of 3-oxo-C12 and 3-oxo-C12:2 AHLs on paracellular permeability in Caco-2/TC7 cells in basal or inflammatory conditions. (a) Paracellular permeability to macromolecules assessed by the passage from the apical to the basal side of FITC-Dextran 4kDa (FD4) upon apical exposure to each AHL (150 µM, 48 h) or basal exposure to IFNγ+TNFα (50 ng/mL, 48 h). Treatments were performed individually or in combination as indicated. Results are expressed as percentage of the initial quantity of tracer (mean ± SEM of triplicates from 9 independent experiments, Kruskall-Wallis test ****P < .0001). (b) Paracellular permeability to ions assessed by the transepithelial electrical resistance (TEER). Treatments were as in (a) (mean ± SEM of triplicates from 3 independent experiments, ordinary one-way ANOVA ****P < .0001). (c) Paracellular permeability to macromolecules assessed by the passage of FD4 from the apical to the basal side of the Caco-2/TC7 cells treated on their apical side with each AHL (150 µM, 48 h) and co-cultured with activated monocytic THP-1 cells added in the basal compartment for the last 24 h of the experiment (mean ± SEM of triplicates from 2 independent experiments, Kruskall-Wallis test **P < .01). For a,band c, respective Holm-Sidak's or Dunn's posttests: **P < .01, ****P < .0001 *vs*. control; $^{\#}$P < .05, $^{\#\#}$P < .01, $^{\#\#\#}$P < .001, $^{\#\#\#\#}$P < .0001 *vs*. indicated conditions. C12 stands for 3-oxo-C12 and C12:2 stands for 3-oxo-C12:2.

triggered a 30-fold rise in FD4 flux in the co-culture, 3-oxo-C12:2 AHL did not modify THP-1 effects on FD4 passage.

Thus, our results confirmed the deleterious role of 3-oxo-C12 AHL on the epithelial barrier function and further demonstrated that it can synergize with another detrimental stimulus such as pro-inflammatory cytokines, whereas 3-oxo-C12:2 remained harmless.

Cell death contributes to intestinal hyperpermeability under inflammatory conditions, generating a TJ-independent unrestricted pathway.[41] We assessed cell cytotoxicity through the lactate dehydrogenase (LDH) release in the presence of AHLs, combined with IFNγ+TNFα or in co-culture experiments. The treatment with AHLs alone did not induce significant cytotoxicity in Caco-2/TC7 cells. The increase of LDH release observed in the presence of IFNγ+TNFα alone (2.3-fold, Supplementary Figure 1B) was not further modified when 3-oxo-C12:2 AHL was added. In combination with 3-oxo-C12, the increase in LDH release was slightly greater (3-fold), but without statistic difference. Interestingly, in Caco-2/TC7 cells co-cultured with THP-1 monocytes, the only increase in LDH release was observed upon 3-oxo-C12 treatment (2.3-fold, Supplementary Figure 1 C). Taken together, these results showed that the effects of AHLs on permeability were only partially concordant with the cytotoxicity measured in the different conditions. This suggested that cell death was likely to participate in the increase in paracellular permeability in the presence of IFNγ+TNFα, but that other mechanisms concomitantly contributed to the differential effects of the two AHLs on the barrier function.

3-oxo-C12:2 AHL protects tight junctions from IFNγ and TNFα deleterious effects

Tight junctions (TJ) seal the paracellular space and thus control the flux of molecules or solutes between adjacent cells. We thus investigated whether TJ reorganization accompanied the effects described above on paracellular permeability. Representative images of immunofluorescence staining (Figure 3a), and quantification of the fluorescence (Figure 3(b,c)), showed that treatment with 3-oxo-C12 AHL alone tended to reduce the signal of both transmembrane proteins occludin (Figure 3(a,b)), −19% vs control) and tricellulin (Figure 3(a,c)), −16% vs control), respectively at bicellular or tricellular cell contacts. On the contrary, in the presence of 3-oxo-C12:2, occludin or tricellulin staining remained similar to control (Figure 3(a,b,

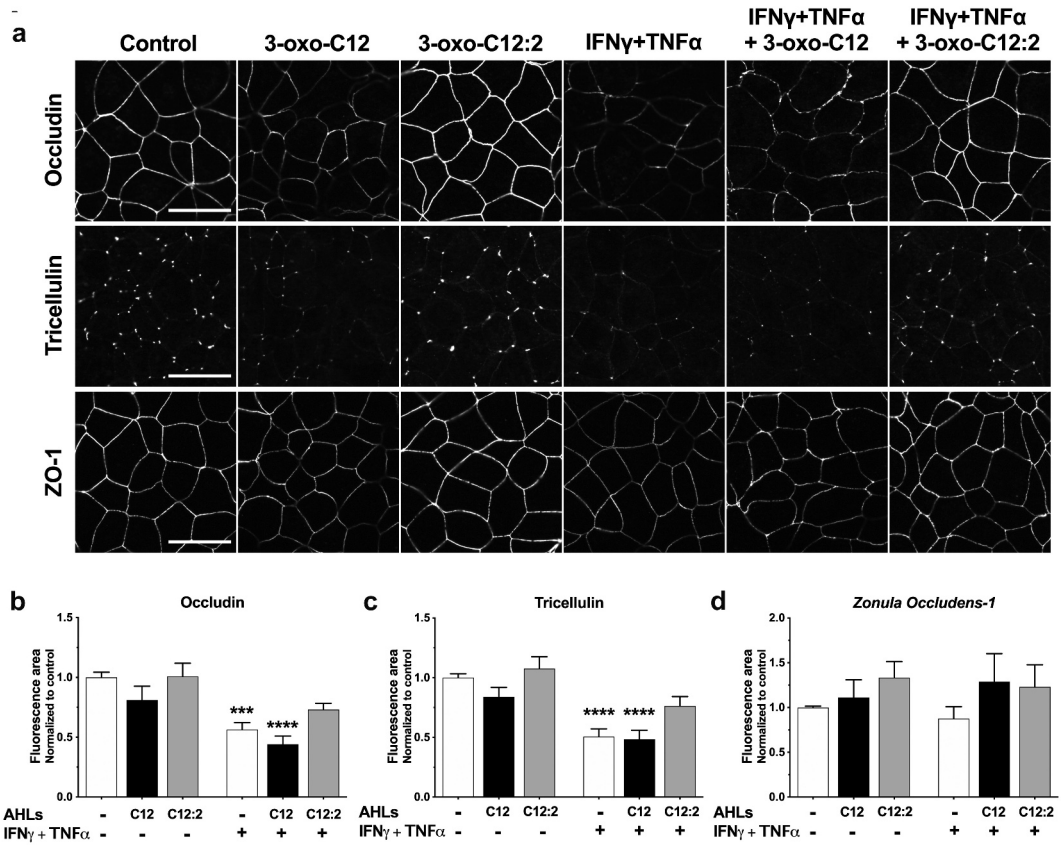

Figure 3. Opposite effects of 3-oxo-C12 and 3-oxo-C12:2 AHLs on tight junction proteins. (a) Representative fields of structured illumination microscopy images from immunofluorescence of occludin (bicellular contacts), tricellulin (tricellular junctions) and Zonula Occludens-1 (ZO-1) upon apical exposure of Caco-2/TC7 cells to each AHL (150 µM, 48 h) and/or basal exposure to IFNγ+TNFα (50 ng/mL, 48 h). Scale bar: 20 µm. **(b,c,d)** Quantification of immunofluorescence staining area of occludin (b, mean ± SEM of duplicates from 5 independent experiments, ordinary one-way ANOVA ****P < .0001), tricellulin (c, mean ± SEM of duplicates from 4 independent experiments, ordinary one-way ANOVA ****P < .0001) and Zonula Occludens-1 (ZO-1) (d, mean ± SEM of duplicates from 3 independent experiments, Kruskall-Wallis test $P = .3$). Forband c, Holm-Sidak's post tests: *** $P < .001$ and **** $P < .0001$ *vs*. control. C12 stands for 3-oxo-C12; C12:2 stands for 3-oxo-C12:2.

c)), confirming an absence of deleterious effect on the barrier function.

Upon exposure to IFNγ+TNFα, signals at cell-contacts were significantly decreased compared to control for occludin (Figure 3(a,b), −44%) and tricellulin (Figure 3(a,c), −50%), and this effect was maintained to a comparable extent in combination with 3-oxo-C12 (occludin −56% and tricellulin −52%). More importantly, 3-oxo-C12:2 AHL partially prevented the cytokine-induced decrease in fluorescence for occludin (Figure 3(a,b)), −27% *vs*. −44% with cytokines only) as well as for tricellulin (Figure 3(a,c), −24% *vs*. −50% with cytokines only).

We then analyzed *Zonula Occludens*-1 (ZO-1), which is the main cytoplasmic partner of transmembrane TJ proteins. Interestingly, in the presence of 3-oxo-C12 AHL with or without cytokines, only a slight decrease in ZO-1 staining was observed, which was much less pronounced than for transmembrane TJ proteins (Figure 3a), and modifications between conditions did not reach statistical differences (Figure 3d). ZO-1 staining was maintained in presence of 3-oxo-C12:2 AHL. In addition, the transmembrane protein E-Cadherin, forming adherens junctions, was partially mislocalized (identified as intracellular puncta) in the presence of 3-oxo-C12 AHL or IFNγ+TNFα, individually or in combination (Supplementary Figure 2). Conversely, 3-oxo-C12:2 AHL preserved E-Cadherin at cell-cell contacts and abolished cytokine-induced mislocalization (Supplementary Figure 2). Thanks to E-cadherin staining, which delineates cell contours,

irregular epithelial morphology was observed in the presence of cytokines as expected, whereas the regular cobblestone shape of Caco-2/TC7 was maintained with 3-oxo-C12:2.

Collectively, these data confirmed in Caco-2/TC7 intestinal cells previous studies showing impairment of tight junctions by the 3-oxo-C12 AHL alone. We further showed that 3-oxo-C12 did not modulate the deleterious effects of pro-inflammatory cytokines on intercellular junctions, whereas we highlighted for the first time a protective role of 3-oxo-C12:2 AHL, notably on the bicellular TJ protein occludin and tricellular TJ protein tricellulin.

3-oxo-C12:2 AHL maintains TJs protein complexes in presence of cytokines contrary to 3-oxo-C12 AHL

To better understand at what level of TJ regulation the effects of AHLs occured, we first determined whether mRNA levels of genes encoding TJ proteins and/or total protein levels were modified in response to AHLs and cytokines. Our results showed that upon IFNγ+TNFα exposure, mRNA levels of both occludin and tricellulin tended to be decreased (*OCLN*, Figure 4a, *MARVELD2*, Figure 4b), as well as their total protein levels (Figure 4(d,f,g)). This tendency was maintained in combination with both AHLs without any distinct effects of each molecule compared to cytokines only (Figure 4(a,b,d,e,f,g)). It is worth noting that exposure to 3-oxo-C12:2 alone induced a slight increase in occludin mRNA levels (Figure 4a, 1.3-fold) and a similar tendency for tricellulin (Figure 4b, 1.3-fold), whereas 3-oxo-C12 AHL did not. In addition, ZO-1 gene mRNA levels (*TJP1*, Figure 4c) and ZO-1 total protein levels (Figure 4(d,h)) remained unchanged in all conditions. Similarly, E-Cadherin levels were not modified (Figure 4(d,e)).

Although the pore pathway was less impacted than the leak pathway in our conditions, the expression of several claudins was analyzed. The level of the sealing claudin-7 mRNA was not significantly modified by pro-inflammatory cytokines, that of the sealing claudin-4 tended to be increased and the pore-forming claudin-2 was decreased (Supplementary Figure 3). As with occludin and tricellulin, the presence of either AHL did not significantly modulate cytokine effects on mRNA levels of claudin genes.

Overall, pro-inflammatory cytokines IFNγ+TNFα tended to downregulate the expression of TJ proteins involved in the leak pathway, in accordance with the data from immunofluorescence analyses. The results showed that 3-oxo-C12:2, which partially prevented the decrease in occludin and tricellulin signal at cell-contacts caused by cytokines (Figure 3), did not modulate their effects on mRNA or total protein levels. We thus hypothesized that protective effects exerted by this AHL could occur through the regulation of TJ stability at cell-cell contacts.

In order to study TJ protein complexes, we used the Duolink proximity ligation assay (PLA) to visualize *in situ* specific endogenous protein–protein interactions. We analyzed interactions between occludin and its cytoplasmic partner ZO-1 on one hand, and between tricellulin and ZO-1 on the other hand.

In untreated Caco-2/TC7 cells, PLA spots of occludin/ZO-1 interaction appeared as fluorescent punctate labeling at bicellular cell-cell contacts (Figure 5a, upper panel) thus recapitulating TJ network. Treatment with 3-oxo-C12 AHL alone led to a decreased number of PLA spots of occludin/ZO-1 compared to control, while 3-oxo-C12:2 AHL did not seem to affect by itself the interaction between these proteins. In the presence of cytokines IFNγ+TNFα, the density of occludin/ZO-1 PLA spots was diminished and this decrease was maintained in combination with 3-oxo-C12 AHL. When 3-oxo-C12:2 AHL was combined with cytokines, the pattern observed was strikingly different since a very intense network of PLA spots delineating cell-cell contacts was maintained.

In order to objectify our qualitative observations, we estimated the number of occludin/ZO-1 PLA spots (Figure 5b). A strong trend toward reduced counts of occludin/ZO-1 PLA spots was observed upon exposure to IFNγ+TNFα (−55% *vs.* control) or in co-treatment with 3-oxo-C12 (−46% *vs.* control). In accordance with the microscopy observations, quantification confirmed a significant preventing effect of 3-oxo-C12:2 AHL against the cytokine-induced drop of occludin/ZO-1 PLA spots.

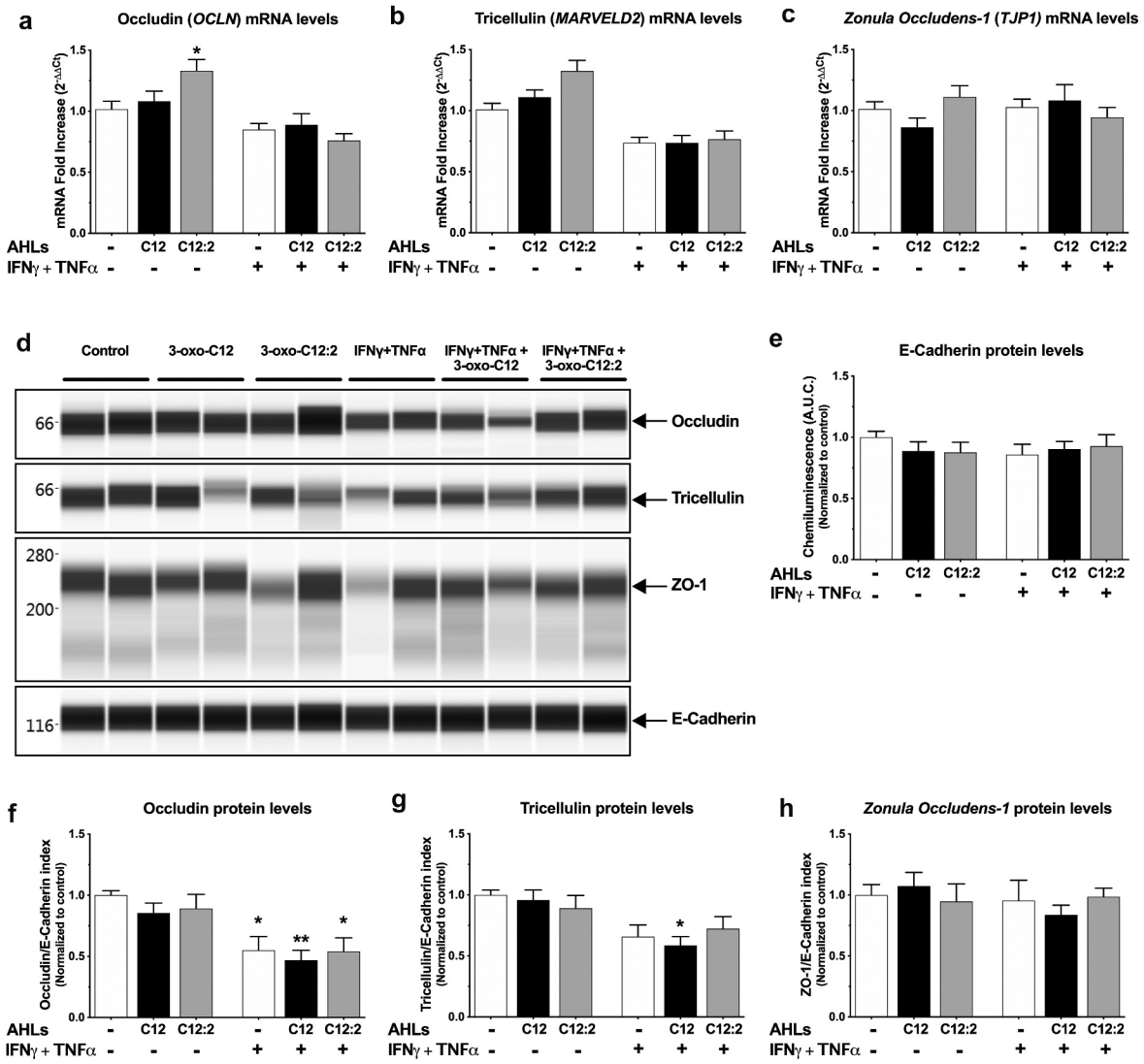

Figure 4. mRNA and total protein levels of occludin, tricellulin and ZO-1 upon exposure to each AHL in basal or inflammatory conditions. Caco-2/TC7 cells were treated on their apical side by each AHL (150 µM, 48 h) or on their basal side by IFNγ+TNFα (50 ng/mL, 48 h). Treatments were performed individually or in combination as indicated. **(a, b, c)** mRNA levels were determined by (RT)-qPCR for occludin gene (*OCLN*) (a, ordinary one-way ANOVA ****P < .0001), tricellulin gene (*MARVELD2*) (b, Kruskall-Wallis test ****P < .0001) and Zonula Occludens-1 gene (*TJP1*) (c, ordinary one-way ANOVA $P = .36$). Results are expressed as $2^{-\Delta\Delta Ct}$ using cyclophylin as the house keeping gene (mean ± SEM of triplicates from 3 independent experiments). (d) Total protein levels of occludin, tricellulin and Zonula Occludens-1 and E-cadherin were quantified by Wes ™ capillary electrophoresis. Reconstructed images are displayed, based on the area under the curve from chemiluminescence signal obtained for one experiment (representative of 3 independent experiments). Molecular weight markers (in kDa) are indicated on the left. (e) Total E-cadherin protein levels (Areas under the curve from chemiluminescence results, ordinary one-way ANOVA $P = .82$). **(f, g, h)** Total protein levels of occludin (f, ordinary one-way ANOVA ***P < .001), tricellulin (g, ordinary one-way ANOVA **P < .01), and ZO-1 (h, ordinary one-way ANOVA $P = .8$): areas under the curve from chemiluminescence results are normalized to respective E-Cadherin levels, which do not differ between conditions (e), and expressed as ratio values normalized to the control condition (mean ± SEM of duplicates from 3 independent experiments). For a-c and e-h, respective Holm-Sidak's or Dunn's posttests * $P < .05$ and ** $P < .01$ *vs*. control. C12 stands for 3-oxo-C12; C12:2 stands for 3-oxo-C12:2.

Being representative of tricellulin localization pattern, PLA spots of tricellulin/ZO-1 interaction were mostly visualized in untreated cells at tricellular cell-cell contacts and more sporadically at bicellular junctions (Figure 5a, bottom panel). In the presence of 3-oxo-C12 AHL alone, PLA spots of tricellulin/ZO-1 were less dense compared to control, while treatment with 3-oxo-C12:2 did not modify the density or localization of tricellulin/ZO-1 PLA spots (Figure 5a). Interestingly, in

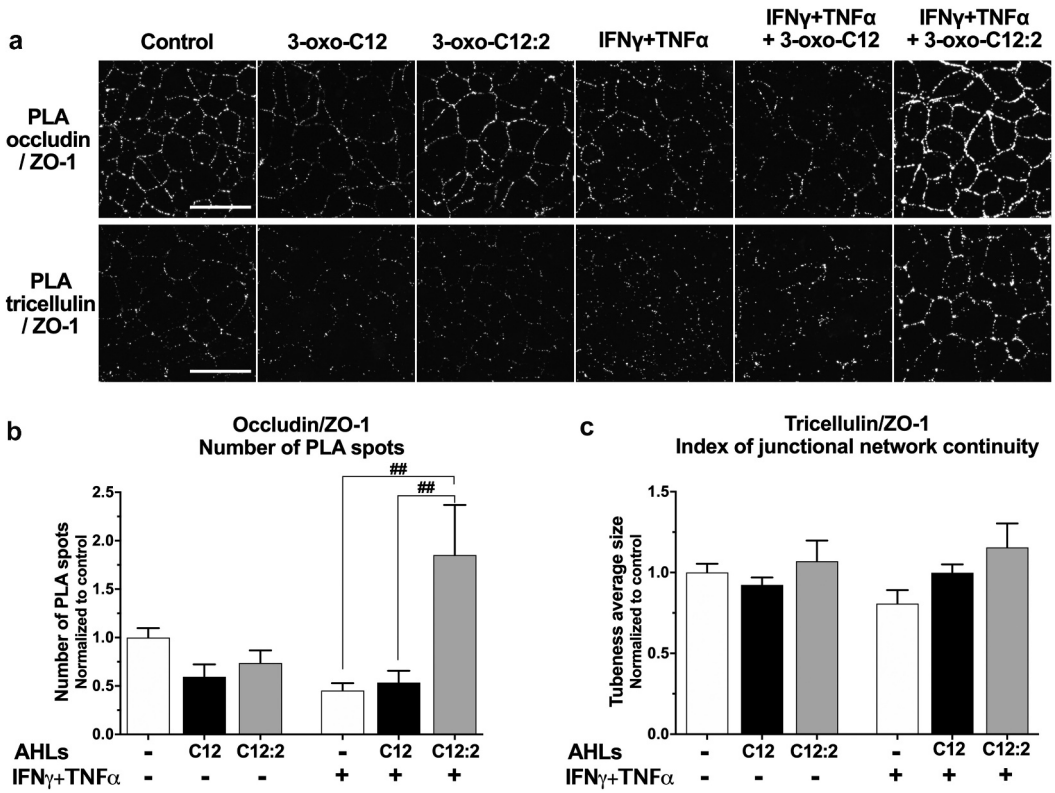

Figure 5. The 3-oxo-C12:2 AHL maintains interaction of occludin and tricellulin with their cytoplasmic partner Zonula Occludens-1 under inflammatory conditions. Caco-2/TC7 cells were treated as in Figures 2 and 3 and interactions between TJ proteins were analyzed by Proximity Ligation Assay (PLA) (a) Representative fields of structured illumination microscopy images from PLA (white spots) between occludin and *Zonula Occludens*-1 (ZO-1) (top) or between tricellulin and ZO-1 (bottom). Scale bar: 20 µm. (b) Quantification of Occludin/ZO-1 PLA spots (mean ± SEM of 2 or 3 replicates from 3 independent experiments, ordinary one-way ANOVA **P < .01, Holm-Sidak's posttests: $^{\#\#}$P < .01 *vs*. indicated conditions). (c) Quantification of the *tubeness* average size of Tricellulin/ZO-1 PLA spots, as an index of junctional network continuity (mean ± SEM of 2 or 3 replicates from 3 independent experiments, ordinary one-way ANOVA $P = .23$). C12 stands for 3-oxo-C12; C12:2 stands for 3-oxo-C12:2.

response to IFNγ+TNFα only or in association with 3-oxo-C12, the density of tricellulin/ZO-1 PLA spots did not seem changed but their spatial distribution was modified and they appear less organized and more scattered throughout the cells compared to control (Figure 5a, lower panel). By contrast, when 3-oxo-C12:2 AHL was added to cytokine-treated cells, the density and distribution of tricellulin/ZO-1 PLA spots were not affected compared to control, and were preserved from cytokine-triggered scattering. To objectify the dispersal of tricellulin/ZO-1 complexes, we analyzed the continuity of junctional networks formed by PLA spots (Figure 5c). Although no statistical difference arose, the analysis showed that IFNγ+TNFα tended to disperse tricellulin/ZO-1 complexes and that 3-oxo-C12:2 AHL prevented this disorganization.

Taken together, these data showed that 3-oxo-C12 AHL disrupted TJ complexes, but without synergistic effects with cytokines. More importantly 3-oxo-C12:2 AHL prevented TJ disruption caused by pro-inflammatory cytokines by maintaining interactions between occludin or tricellulin with their main cytoplasmic partner ZO-1 and the proper localization of complexes at cell-cell contacts.

3-oxo-C12:2 AHL limits cytokine-induced ubiquitination of occludin and tricellulin

To go further, we investigated pathways involved in TJ stabilization that could be targeted by 3-oxo-C12:2 AHL and partake in its protective effects against cytokine damages. The two well-characterized pathways mediating TJ disruption in response to

pro-inflammatory cytokines IFNγ and TNFα involve an enhanced expression of the Myosin Light Chain Kinase (MLCK)[30,41,42] and Rho-associated Kinase (ROCK), which both lead to higher levels of Myosin Light Chain 2 (MLC2) phosphorylation, actin cytoskeleton reorganization and thus internalization of transmembrane TJ proteins.[43–45] We did not find any modulation of either MLCK total protein levels or phosphorylated MLC2/total MLC2 levels (Supplementary Figure 4), and we thus concluded that these pathways were unlikely to be involved in the protective effects of 3-oxo-C12:2 on TJs in presence of cytokines.

Ubiquitination is the most common post-translational modification and the diversity of ubiquitin motifs (the 'ubiquitin code') allows regulation of a wide range of processes including the fate of a cell surface transmembrane protein such as its endocytosis, recycling and degradation.[46,47] Occludin and tricellulin both undergo ubiquitination, which mediates their degradation.[48,49] Hence, we postulated that opposite effects of the two AHLs on TJ integrity could involve pathways regulating their stability at the cell membrane such as their ubiquitin-mediated internalization. We thus determined ubiquitination levels of occludin and tricellulin in Caco-2/TC7 cells, using PLA in order to obtain information on the location of ubiquitinylated proteins (Figure 6a). In control cells, occludin/ubiquitin or tricellulin/ubiquitin PLA spots were scarce and mostly visualized at cell-cell contacts, which were visualized by E-Cadherin staining (Figure 6a, solid line arrows). In addition, a few intracellular PLA spots (close to the plasma membrane) also appeared in both cases (Figure 6a, dashed line arrows). The qualitative and quantitative results showed that in the presence of 3-oxo-C12 alone, but not 3-oxo-C12:2, the number of PLA spots tended to be increased for occludin/ubiquitin (Figure 6b, 1.8-fold increase *vs.* control) and tricellulin/ubiquitin (Figure 6c, 1.7-fold increase *vs.* control). Exposure to IFNγ+TNFα alone led to a 3.2-fold increase in the number of occludin/ubiquitin PLA spots (Figure 6b) and to a 3.5-fold increase in the number of tricellulin/ubiquitin PLA spots (Figure 6c). In co-treatment with 3-oxo-C12, this increase was maintained to a similar extent for tricellulin/ubiquitin PLA spots (Figure 6c), and it was slightly higher for occludin/ubiquitin spots (Figure 6b, 4.2-fold increase *vs.* control). Most importantly, when Caco-2/TC7 cells were exposed to both IFNγ+TNFα and 3-oxo-C12:2, the increase in the number of occludin/ubiquitin PLA spots was totally suppressed (Figure 6b) and the increase in the number of tricellulin/ubiquitin PLA spots was significantly attenuated (Figure 6c).

To reinforce our data, Caco-2/TC7 cells were treated with 3-oxo-C12:2 or IFNγ+TNFα, individually or in co-treatment with the dynamin inhibitor Dynasore, which blocks endocytosis. We postulated that blocking endocytosis would lead to an accumulation of ubiquitinylated occludin or tricellulin at cell-cell contacts. Accordingly, occludin/ubiquitin and tricellulin/ubiquitin PLA spots seemed to be more abundant in control+Dynasore- or in 3-oxo-C12:2+ Dynasore-treated cells (Supplementary Figure 5) than observed without the dynamin inhibitor (Figure 6a). In addition, the increasing effects of IFNγ+TNFα on occludin/ubiquitin and tricellulin/ubiquitin PLA spots number were recapitulated in the presence of Dynasore (Supplementary Figure 5). These observations suggested that under inflammatory conditions, ubiquitination of either occludin or tricellulin at the plasma membrane occurred prior to their internalization and thus mediates their endocytosis.

As a whole, these data clearly showed that pro-inflammatory cytokines IFNγ and TNFα upregulate ubiquitination of the TJ transmembrane proteins occludin and tricellulin. Our results demonstrated that 3-oxo-C12:2 can abolish or attenuate these deleterious effects of cytokines on occludin and tricellulin, thus supporting our initial hypothesis that this new AHL stabilizes transmembrane TJ proteins at the plasma membrane.

3-oxo-C12:2 AHL restrains the interaction between the ubiquitin-ligase itch and occludin or tricellulin

Occludin and tricellulin are both targets of the ubiquitin-ligase itch,[48,49] which is known to ubiquitinate several cell-surface proteins and to mediate their endocytosis.[50] Therefore, we sought to study the interaction between itch and occludin or tricellulin in response to 3-oxo-C12:2 AHL alone and in the presence of cytokines, using PLA since this technique allows to visualize transient interactions. Microscopy images in

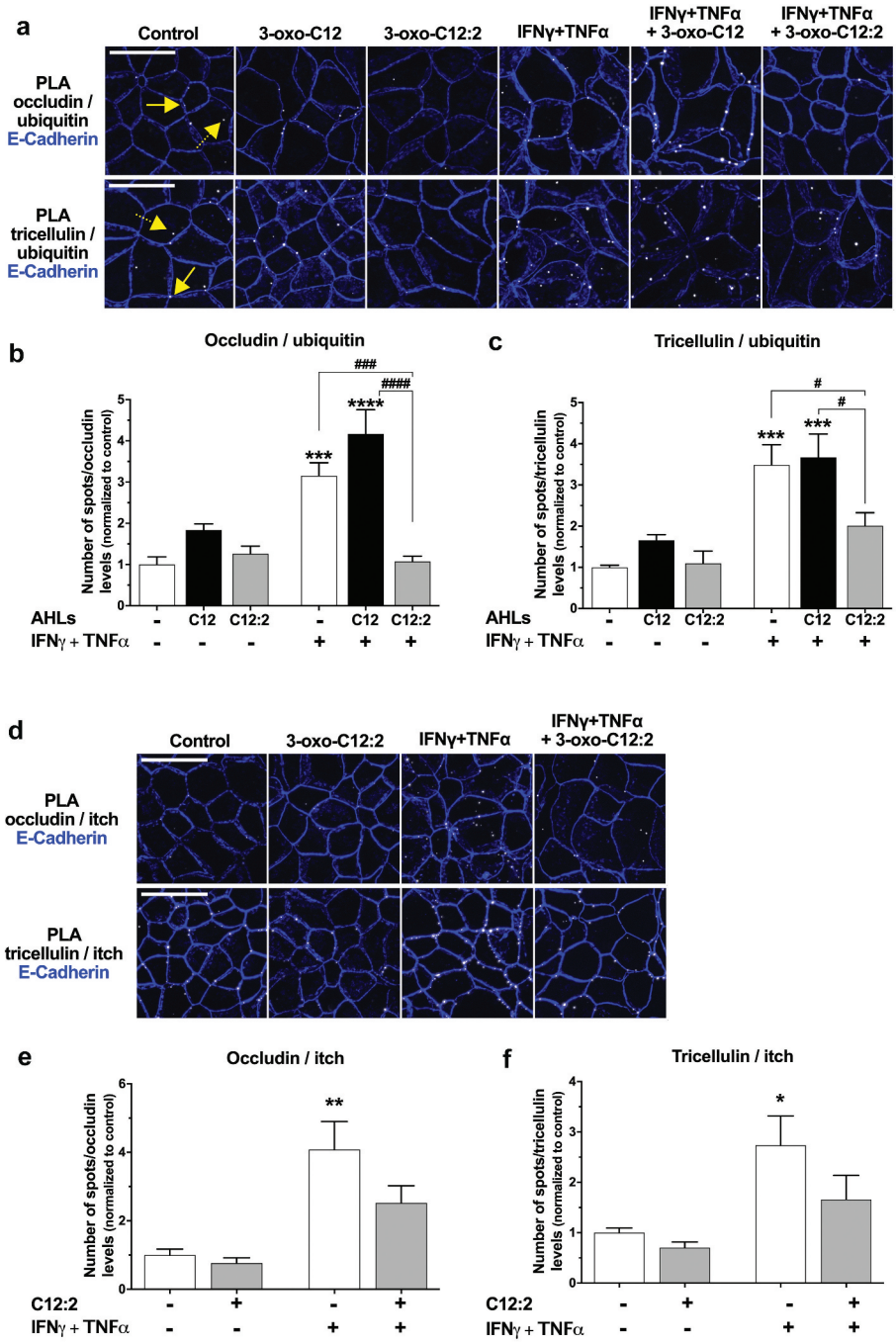

Figure 6. The 3-oxo-C12:2 AHL protects occludin and tricellulin from ubiquitination induced at the plasma membrane in presence of pro-inflammatory cytokines. Caco-2/TC7 cells were treated on their apical side by each AHL (150 µM, 48 h) or on their basal side by IFNγ+TNFα (50 ng/mL, 48h). Treatments were performed individually or in combination as indicated. (a-c) Ubiquitination levels of occludin or tricellulin were determined by Proximity Ligation Assay (PLA). (a) Representative fields of structured illumination microscopy images of PLA (white spots) between occludin and ubiquitin (top) or between tricellulin and ubiquitin (bottom). Cell-cell contacts are visualized by E-Cadherin immunofluorescence staining in blue. The solid line arrows show PLA spots localized at the plasma membrane while dashed line arrows show PLA spots localized within the intracellular space. Scale bar: 20 µm. (b) Quantification of the number of occludin/ubiquitin PLA spots normalized to occludin fluorescence levels. Results are expressed as ratio values normalized to the control condition (mean ± SEM of 2 or 3 replicates from 3 independent experiments, ordinary one-way ANOVA ****P < .0001). (c) Quantification of the number of tricellulin/ubiquitin PLA spots normalized to tricellulin fluorescence levels (mean ± SEM of 2 or 3 replicates from 3 independent experiments, ordinary one-way ANOVA ****P < .0001). (d-f) Interaction of occludin and tricellulin with the ubiquitin-ligase itch was determined by PLA. (d) Representative fields of structured illumination microscopy images from PLA between occludin and itch (top) or between tricellulin and itch (bottom). Cell contacts are visualized by E-Cadherin shown in blue. Scale bar: 20 µm. (e, f) Quantification of the number of occludin/itch PLA spots (e, mean ± SEM of 2 or 3 replicates from 3 independent experiments, ordinary one-way ANOVA ***P < .001) or tricellulin/itch PLA spots (f, mean ± SEM of 2 or 3

untreated cells showed scarce occludin/itch PLA spots, localized at the cell membrane (Figure 6d, upper panel). Interestingly, tricellulin/itch PLA spots were more abundant and were also strictly localized at cell-cell contacts (Figure 6d, lower panel). Microscopy analysis and PLA spots quantifications showed that treatment of cells with 3-oxo-C12:2 AHL alone did not significantly modify PLA spots pattern for occludin/itch (Figure 6(d,e)) or tricellulin/itch (Figure 6(d,f)), although we noticed a trend toward a decrease in their number (respectively −23% and −30% *vs*. control). Conversely, exposure to IFNγ+TNFα alone led to an increase in the number of PLA spots for occludin/itch (Figure 6(d,e), 4-fold increase *vs*. control) and tricellulin/itch interactions (Figure 6d,f) , 2.7-fold increase *vs*. control). Concomitant treatment with 3-oxo-C12:2 AHL attenuated the increase in occludin/itch (Figure 6(d,e)) and tricellulin/itch PLA spots (Figure 6 (d,f)) observed with cytokines.

zInterestingly, no modification of itch localization or itch signal intensity was noticeable in our conditions (data not shown). It is noteworthy that all occludin/itch or tricellulin/itch PLA spots were localized at the cell membrane, including in conditions in which they were more numerous, thus suggesting that the interaction between the ubiquitin-ligase itch and occludin or tricellulin occurred at the plasma membrane and likely prior to internalization of TJ proteins.

Altogether these results suggest that 3-oxo-C12:2 acts on itch-mediated ubiquitination of occludin and tricellulin at cell-cell contacts, before the engagement of these TJ proteins in the endocytic pathway.

Discussion

Acyl-homoserine lactones (AHLs) are the most studied quorum sensing molecules having an impact on host cells, and as such, deserve to be extensively studied in the context of the gut ecosystem. We recently identified a never described AHL, 3-oxo-C12:2, as the most prominent intestinal AHL.[23] The present study reveals a protective role of this molecule against tight junction dysregulation under inflammatory conditions, in contrast with the deleterious effects exerted by the structurally close 3-oxo-C12 AHL produced by the opportunist pathogen *P. aeruginosa*.

Several previous studies demonstrated that 3-oxo-C12 AHL, at doses in the range of concentrations found in biofilms,[37] disrupts epithelial barriers, in particular through alteration of tight junction proteins.[26–29] On the opposite, our previous study showed no impact of 3-oxo-C12:2 on paracellular permeability to macromolecules in Caco-2/TC7 enterocytic cells.[23] While it is well known that different N-acyl-homoserine lactones with varying acyl chain length exhibit distinct properties,[28,51,52] our group demonstrated the importance of acyl chain insaturations on biological activities.[23] In the present study, we confirm contrasting effects of the two structurally close molecules, and we further show opposite outcomes when mimicking inflammatory conditions encountered in IBD. In presence of a mixture of two pro-inflammatory cytokines IFNγ and TNFα, known to impair tight junction integrity,[30] or in co-culture with activated monocytic cells, the 3-oxo-C12 AHL from *P. aeruginosa* dramatically amplifies hyperpermeability. It is worth noting that the synergistic effect of 3-oxo-C12 and proinflammatory cytokines occurs on permeability to macromolecules (passage of dextran 4 kDa) and, to a lesser extent, to smaller molecules (passage of sulfonic acid 0.4 kDa), but not on permeability to ions (TEER). This is in accordance with the loss of occludin and tricellulin at tight junctions, since these two proteins are known to control the leak pathway.[6,7] In full opposition, the newly described 3-oxo-C12:2 AHL clearly preserves occludin and tricellulin at tight junctions under inflammatory conditions but without improving epithelial permeability to either macromolecules or ions (Figure 7).

replicates from 3 independent experiments, ordinary one-way ANOVA **P < .01). Numbers of PLA spots are reported to occludin or tricellulin fluorescence levels and results are expressed as ratio values normalized to the control condition. For b, c,eand f, Holm-Sidak's post tests: *P < .05, **P < .01, ***P < .001, ****P < .0001 *vs*. control; $^{\#}$P < .05, $^{\#\#\#}$P < .001, $^{\#\#\#\#}$P < .0001 *vs*. indicated conditions. C12 stands for 3-oxo-C12; C12:2 stands for 3-oxo-C12:2.

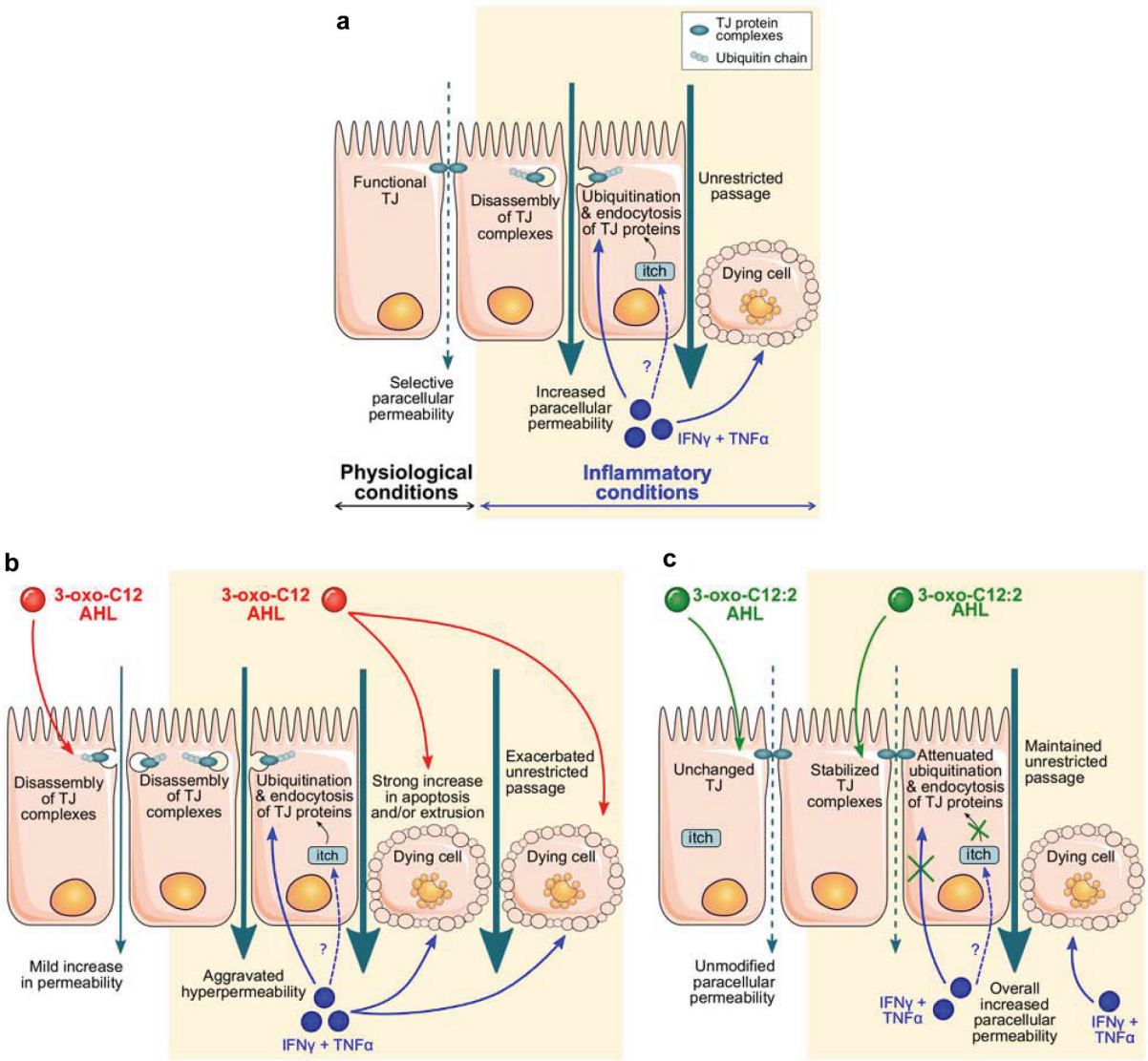

Figure 7. Proposed mechanisms explaining the distinct effects of 3-oxo-C12 and 3-oxo-C12:2 AHLs on the intestinal epithelial barrier under basal or inflammatory conditions. (a) In physiological conditions (left), tight junctions (TJ) seal the paracellular space between intestinal epithelial cells and control paracellular permeability in a selective manner. Under inflammatory conditions (right), recapitulated by IFNγ and TNFα exposure, interactions between TJ proteins are destabilized. Pro-inflammatory cytokines induce an increase in the interaction of the E3-ligase itch with TJ proteins, which undergo higher ubiquitination and are internalized. These events lead to increased paracellular permeability. How cytokines regulate itch interaction with TJ proteins remains to be determined (dashed arrow and question mark). In addition, cytokines induce a moderate rate of cell death, which participates in hyperpermeability through the TJ-independent unrestricted pathway. (b) Exposure to 3-oxo-C12 AHL alone (left) alters TJ integrity and induces a mild increase in permeability. Under inflammatory conditions (right), 3-oxo-C12 AHL does not further impair TJ but aggravates cytokine-induced cell death, hence drastically exacerbating the increase in permeability. (c) Presence of 3-oxo-C12:2 AHL alone (left) does not impair TJ structure and does not modify paracellular permeability. Under inflammatory conditions (right), 3-oxo-C12:2 AHL stabilizes TJ by tempering the dismantling of TJ protein complexes. In addition, while the permeability remains elevated through the unrestricted pathway, this AHL limits the interaction between TJ proteins and itch and attenuates the increased ubiquitination of TJ proteins, thus preventing their endocytosis.

In IBD, ulceration and epithelial apoptosis contribute to disruption of the intestinal barrier.[14,53] In addition to damaging tight junctions, pro-inflammatory cytokines such as TNFα – through activation of their receptor – trigger epithelial cell apoptosis and generate a tight junction-independent unrestricted pathway.[41] As expected, given the cytokine treatment we used, a moderate cytotoxicity evaluated by LDH release was observed and was likely to

contribute to the increased permeability to macromolecules besides tight junction opening. Remarkably, 3-oxo-C12 or 3-oxo-C12:2 AHLs had very distinctive effects on cytokine-induced unrestricted pathway. We hypothesized that the drastic increase in macromolecule permeability induced by the combination of cytokines and 3-oxo-C12 was due to increased cell death since we showed that tight junctions were not synergistically damaged. Accordingly, 3-oxo-C12 AHL and cytokines both induced apoptosis in the Caco-2/TC7 monolayer and the aggravating effect of 3-oxo-C12 on cytokine-induced hyperpermeability was completely abolished in the presence of a large spectrum caspase inhibitor (data not shown). We thus concluded that cell death was responsible for the synergistic effects of cytokines and 3-oxo-C12 (Figure 7b), in accordance with studies showing that this AHL induces apoptosis in several cell types.[52,54,55] Regarding 3-oxo-C12:2, this AHL did not prevent cytokine-induced hyperpermeability, despite clear protective effects on TJ integrity and stability. Given that this AHL decreased neither cell toxicity nor apoptosis induced by cytokines (not shown), we assume that cell death hid beneficial effects of TJ-protecting 3-oxo-C12:2 AHL on epithelial permeability (Figure 7c).

We focused our study on two tight junction-associated MARVEL proteins (TAMPs) known to control the leak pathway: occludin and tricellulin and their cytoplasmic partner ZO-1. Although 3-oxo-C12 AHL did not quantitatively decrease signal of TJ proteins, their junctional localization was slightly altered by the molecule, in accordance with previous studies.[26,28] Both occludin and tricellulin were diminished at cell-cell junctions in response to IFNγ and TNFα, as expected. On the contrary, the junctional localization of ZO-1 was much less affected and ZO-1 protein content remained unchanged unlike the two transmembrane proteins occludin and tricellulin, whose total levels were decreased upon cytokine treatment. These results may be explained by the fact that ZO-1 could be present at the plasma membrane through its interaction with many other transmembrane junctional proteins, several of which are probably not – or less – affected in our conditions. Despite the apparent lack of perturbation of the whole ZO-1 pool, our PLA experiments showed that molecular complexes involving occludin and ZO-1 were greatly decreased in response to 3-oxo-C12 AHL and/or cytokines. Complexes involving tricellulin and ZO-1 were spatially scattered, suggesting disorganized tricellular TJ. A striking effect of 3-oxo-C12:2 AHL was the conservation of occludin or tricellulin interaction with ZO-1 at the plasma membrane and the correct spatial distribution of these two different complexes, supporting a preserved barrier. While little is known about the functional outcome of tricellulin/ZO-1 complex, the occludin interaction with ZO-1 has been shown to regulate occludin trafficking, localization at the plasma membrane and its barrier function.[56,57]

Increased endocytosis is an important mechanism involved in junction disassembly during intestinal inflammation.[4] Internalization of cell-surface proteins – including transmembrane TJ proteins[58] – involves several pathways leading to either their recycling or degradation. In addition, ubiquitination is a crucial post-translational modification of transmembrane proteins regulating their endocytosis, trafficking and ultimately their cell surface level.[46,47] Phosphorylation of several TJ proteins including occludin[59] has been associated with their ubiquitination.[60] Here, we show that IFNγ and TNFα increased the proportion of ubiquitinated molecular complexes involving occludin and tricellulin. The accumulation of such complexes at the plasma membrane upon endocytosis inhibition supports our hypothesis that ubiquitination of occludin and tricellulin occurs at cell-cell contacts and probably mediates their endocytosis. We further demonstrate for the first time that these cytokines promote interaction at cell–cell contacts of both TAMPs with itch, identifying this E3-ubiquitin ligase as a potential new actor in the signaling pathways involved in junction disassembly under inflammatory conditions. The 3-oxo-C12:2 AHL can modulate these interactions, and we propose that the down-regulation of itch-mediated occludin and tricellulin ubiquitination stabilizes both proteins together with their molecular partners at the cell membrane, a mechanism that could explain

the AHL protective effects on TJ integrity and stability (Figure 7c). The molecular pathways through which 3-oxo-C12:2 can modulate the ubiquitination process remain to be determined. The identification of eukaryotic AHL interactant proteins is a challenging objective. Among the mammalian interactants of the *P. aeruginosa*-produced 3-oxo-C12 AHL that have been so far identified, are the IQ-motif-containing GTPase-activating protein IQGAP1,[61] the peroxisome proliferator-activated receptors (PPARs),[62] as well as the bitter receptor T2R38.[63] In future studies, the identification of 3-oxo-C12:2 specific eukaryotic targets will allow to further decipher its mechanisms of action, a strategy used in a previous study using biotinylated 3-oxo-C12.[61]

We previously demonstrated that 3-oxo-C12:2 AHL is lost in IBD patients, especially during flare.[23] Further studies will be needed to integrate all the properties of this new AHL in the context of the gut ecosystem, including its possible impact on the microbiota composition as well as its anti-inflammatory activity.[23] Our new findings showing that 3-oxo-C12:2 is able to limit tight junction dismantling in epithelial cells exposed to an inflammatory environment may have therapeutic perspectives in dysfunction of the intestinal barrier in IBD.

Abbreviations:

TJ	tight junctions;
AHL	N-acyl homoserine lactones;
IFNγ	Interferon-γ;
TNFα	Tumor Necrosis Factor-α;
ZO-1	Zonula Occludens-1;
SCFA	short chain fatty acids;
IBD	inflammatory bowel disease;
CD	Crohn's disease;
QS	quorum sensing;
FD4	FITC-Dextran 4 kDa;
TEER	transepithelial electrical resistance;
LDH	lactate dehydrogenase;
PLA	Proximity ligation assay;
DAPI	4′ -6-diamidino-2-phenylindole;
MLCK	Myosin Light Chain Kinase;
ROCK	Rho Associated Kinase;
MLC2	Myosin Light Chain 2;
TAMPs	Tight junction Associated MARVEL Proteins;
IQGAP1	IQ-motif-containing GTPase-activating protein;
PPAR	peroxisome proliferator-activated receptor

Acknowledgments

We would like to thank Frédérick Barreau for numerous advice, Jean-Pierre Hugot and Maryline Roy for THP-1 cells, Agathe Peyrottes for her help on chemistry points and for providing many answers to our questions thanks to her work, Jean-Maurice Mallet for advice and perspectives on the project, Marielle Moreau for support in WES analysis, Céline Prunier for itch antibody and helpful discussions, Sébastien Léon for precious advice about ubiquitination and strategy. This work was supported by the Association François Aupetit (AFA); Institut National de la Santé et de la Recherche Médicale; Sorbonne Université; Ecole Pratique des Hautes Etudes. DA was the recipient of a fellowship from CORDDIM Ile de France.

Disclosure of interest

Professor Seksik has received personal fees from Takeda, Merck MSD, Biocodex, Ferring, Mayoly Spindler, Astellas, Amgen and Abbvie but has no conflict of interest linked to this work. The remaining authors disclose no conflict.

Funding

THIS WORK WAS SUPPORTED BY THE INSERM; ASSOCIATION FRANÇOIS AUPETIT; CORDDIM ILE DE FRANCE; SORBONNE UNIVERSITE; EPHE.

ORCID

Barbara G. Postal http://orcid.org/0000-0002-6505-2018
Céline Osinski http://orcid.org/0000-0003-4897-8510
Daniel Stockholm http://orcid.org/0000-0002-5069-5256
Véronique Carrière http://orcid.org/0000-0002-6263-0847
Sophie Thenet http://orcid.org/0000-0002-0336-2942

References

1. Laukoetter MG, Bruewer M, Nusrat A. Regulation of the intestinal epithelial barrier by the apical junctional complex. Curr Opin Gastroenterol. 2006;22:85–89. doi:10.1097/01.mog.0000203864.48255.4f.
2. Buckley A, Turner JR. Cell biology of tight junction barrier regulation and mucosal disease. Cold Spring Harb Perspect Biol. 2018;10:a029314.doi: 10.1101/cshperspect.a029314.
3. Zihni C, Mills C, Matter K, Balda MS. Tight junctions: from simple barriers to multifunctional molecular gates. Nat Rev Mol Cell Biol. 2016;17:564–580. doi:10.1038/nrm.2016.80.

Lechuga S, Ivanov AI. Disruption of the epithelial barrier during intestinal inflammation: quest for new molecules and mechanisms. Biochim Biophys Acta Mol Cell Res. 2017;1864:1183–1194. doi:10.1016/j.bbamcr.2017.03.007.

5. Shen L, Weber CR, Raleigh DR, Yu D, Turner JR. Tight junction pore and leak pathways: a dynamic duo. Annu Rev Physiol. 2011;73(1):283–309. doi:10.1146/annurev-physiol-012110-142150.
6. Al-Sadi R, Khatib K, Guo S, Ye D, Youssef M, Ma T. Occludin regulates macromolecule flux across the intestinal epithelial tight junction barrier. Am J Physiol Gastrointest Liver Physiol. 2011;300:G1054–64. doi:10.1152/ajpgi.00055.2011.
7. Krug SM, Amasheh S, Richter JF, Milatz S, Gunzel D, Westphal JK, Huber O, Schulzke JD, Fromm M. Tricellulin forms a barrier to macromolecules in tricellular tight junctions without affecting ion permeability. Mol Biol Cell. 2009;20(16):3713–3724. doi:10.1091/mbc.e09-01-0080.
8. Odenwald MA, Turner JR. Intestinal permeability defects: is it time to treat? Clin Gastroenterol Hepatol. 2013;11:1075–1083. doi:10.1016/j.cgh.2013.07.001.
9. Neurath MF. Cytokines in inflammatory bowel disease. Nat Rev Immunol. 2014;14:329–342. doi:10.1038/nri3661.
10. Luissint AC, Parkos CA, Nusrat A. Inflammation and the intestinal barrier: leukocyte-epithelial cell interactions, cell junction remodeling, and mucosal repair. Gastroenterology. 2016;151:616–632. doi:10.1053/j.gastro.2016.07.008.
11. Hollander D, Vadheim CM, Brettholz E, Petersen GM, Delahunty T, Rotter JI. Increased intestinal permeability in patients with Crohn's disease and their relatives. A possible etiologic factor. Ann Intern Med. 1986;105:883–885. doi:10.7326/0003-4819-105-6-883.
12. Keita AV, Lindqvist CM, Ost A, Magana CDL, Schoultz I, Halfvarson J. Gut barrier dysfunction-a primary defect in twins with Crohn's disease predominantly caused by genetic predisposition. J Crohns Colitis. 2018;12:1200–1209. doi:10.1093/ecco-jcc/jjx180.000.
13. Wyatt J, Vogelsang H, Hubl W, Waldhoer T, Lochs H. Intestinal permeability and the prediction of relapse in Crohn's disease. Lancet. 1993;341:1437–1439. doi:10.1016/0140-6736(93)90882-H.
14. Zeissig S, Burgel N, Gunzel D, Richter J, Mankertz J, Wahnschaffe U, Kroesen AJ, Zeitz M, Fromm M, Schulzke J-D, et al. Changes in expression and distribution of claudin 2, 5 and 8 lead to discontinuous tight junctions and barrier dysfunction in active Crohn's disease. Gut. 2007;56:61–72. doi:10.1136/gut.2006.094375.
15. Krug SM, Bojarski C, Fromm A, Lee IM, Dames P, Richter JF, Turner JR, Fromm M, Schulzke J-D. Tricellulin is regulated via interleukin-13-receptor alpha2, affects macromolecule uptake, and is decreased in ulcerative colitis. Mucosal Immunol. 2018;11:345–356. doi:10.1038/mi.2017.52.
16. Vetrano S, Rescigno M, Cera MR, Correale C, Rumio C, Doni A, Fantini M, Sturm A, Borroni E, Repici A, et al. Unique role of junctional adhesion molecule-a in maintaining mucosal homeostasis in inflammatory bowel disease. Gastroenterology. 2008;135(1):173–184. doi:10.1053/j.gastro.2008.04.002.
17. Vivinus-Nebot M, Frin-Mathy G, Bzioueche H, Dainese R, Bernard G, Anty R, Filippi J, Saint-Paul MC, Tulic MK, Verhasselt V, et al. Functional bowel symptoms in quiescent inflammatory bowel diseases: role of epithelial barrier disruption and low-grade inflammation. Gut. 2014;63(5):744–752. doi:10.1136/gutjnl-2012-304066.
18. Martini E, Krug SM, Siegmund B, Neurath MF, Becker C. Mend your fences: the epithelial barrier and its relationship with mucosal immunity in inflammatory bowel disease. Cell Mol Gastroenterol Hepatol. 2017;4(1):33–46. doi:10.1016/j.jcmgh.2017.03.007.
19. Lavelle A, Sokol H. Gut microbiota-derived metabolites as key actors in inflammatory bowel disease. Nat Rev Gastroenterol Hepatol. 2020;17(4):223–237. doi:10.1038/s41575-019-0258-z.
20. Mukherjee S, Bassler BL. Bacterial quorum sensing in complex and dynamically changing environments. Nat Rev Microbiol. 2019;17(6):371–382. doi:10.1038/s41579-019-0186-5.
21. Pacheco AR, Sperandio V. Inter-kingdom signaling: chemical language between bacteria and host. Curr Opin Microbiol. 2009;12(2):192–198. doi:10.1016/j.mib.2009.01.006.
22. Kaper JB, Sperandio V. Bacterial cell-to-cell signaling in the gastrointestinal tract. Infect Immun. 2005;73(6):3197–3209. doi:10.1128/IAI.73.6.3197-3209.2005.
23. Landman C, Grill JP, Mallet JM, Marteau P, Humbert L, Le Balc'h E, Maubert M-A, Perez K, Chaara W, Brot L, et al. Inter-kingdom effect on epithelial cells of the N-Acyl homoserine lactone 3-oxo-C12:2, a major quorum-sensing molecule from gut microbiota. PLoS One. 2018;13:e0202587. doi:10.1371/journal.pone.0202587.
24. Golovkine G, Reboud E, Huber P. Pseudomonas aeruginosa takes a multi-target approach to achieve junction breach. Front Cell Infect Microbiol. 2017;7:532. doi:10.3389/fcimb.2017.00532.
25. Turkina MV, Vikstrom E. Bacteria-host crosstalk: sensing of the quorum in the context of pseudomonas aeruginosa infections. J Innate Immun. 2019;11:263–279. doi:10.1159/000494069.
26. Vikstrom E, Tafazoli F, Magnusson KE. Pseudomonas aeruginosa quorum sensing molecule N-(3 oxododecanoyl)-l-homoserine lactone disrupts epithelial barrier integrity of Caco-2 cells. FEBS Lett. 2006;580:6921–6928.

27. Vikstrom E, Bui L, Konradsson P, Magnusson KE. The junctional integrity of epithelial cells is modulated by Pseudomonas aeruginosa quorum sensing molecule through phosphorylation-dependent mechanisms. Exp Cell Res. 2009;315:313–326. doi:10.1016/j.yexcr.2008.10.044.
28. Eum SY, Jaraki D, Bertrand L, Andras IE, Toborek M. Disruption of epithelial barrier by quorum-sensing N-3-(oxododecanoyl)-homoserine lactone is mediated by matrix metalloproteinases. Am J Physiol Gastrointest Liver Physiol. 2014;306:G992–G1001. doi:10.1152/ajpgi.00016.2014.
29. Vikstrom E, Bui L, Konradsson P, Magnusson K-E. Role of calcium signalling and phosphorylations in disruption of the epithelial junctions by pseudomonas aeruginosa quorum sensing molecule. Eur J Cell Biol. 2010;89:584–597. doi:10.1016/j.ejcb.2010.03.002.
30. Wang F, Graham WV, Wang Y, Witkowski ED, Schwarz BT, Turner JR. Interferon-gamma and tumor necrosis factor-alpha synergize to induce intestinal epithelial barrier dysfunction by up-regulating myosin light chain kinase expression. Am J Pathol. 2005;166:409–419. doi:10.1016/S0002-9440(10)62264-X.
31. Capaldo CT, Nusrat A. Cytokine regulation of tight junctions. Biochim Biophys Acta. 2009;1788:864–871. doi:10.1016/j.bbamem.2008.08.027.
32. Chantret I, Rodolosse A, Barbat A, Dussaulx E, Brot-Laroche E, Zweibaum A. Differential expression of sucrase-isomaltase in clones isolated from early and late passages of the cell line Caco-2: evidence for glucose-dependent negative regulation. J Cell Sci. 1994;107(Pt 1):213–225.
33. Petit CS, Barreau F, Besnier L, Gandille P, Riveau B, Chateau D, Roy M, Berrebi D, Svrcek M, Cardot P, et al. Requirement of cellular prion protein for intestinal barrier function and mislocalization in patients with inflammatory bowel disease. Gastroenterology. 2012;143(1):122–32 e15. doi:10.1053/j.gastro.2012.03.029.
34. Ghezzal S, Postal BG, Quevrain E, Brot L, Seksik P, Leturque A, Thenet S, Carrière V. Palmitic acid damages gut epithelium integrity and initiates inflammatory cytokine production. Biochim Biophys Acta Mol Cell Biol Lipids. 2020;1865(2):158530. doi:10.1016/j.bbalip.2019.158530.
35. Chateau D, Pauquai T, Delers F, Rousset M, Chambaz J, Demignot S. Lipid micelles stimulate the secretion of triglyceride-enriched apolipoprotein B48-containing lipoproteins by Caco-2 cells. J Cell Physiol. 2005;202:767–776. doi:10.1002/jcp.20173.
36. Kravchenko VV, Kaufmann GF, Mathison JC, Scott DA, Katz AZ, Wood MR, Brogan AP, Lehmann M, Mee JM, Iwata K, et al. N-(3-oxo-acyl)homoserine lactones signal cell activation through a mechanism distinct from the canonical pathogen-associated molecular pattern recognition receptor pathways. J Biol Chem. 2006;281(39):28822–28830. doi:10.1074/jbc.M606613200.
37. Charlton TS, de Nys R, Netting A, Kumar N, Hentzer M, Givskov M, Kjellerberg, S. A novel and sensitive method for the quantification of N-3-oxoacyl homoserine lactones using gas chromatography-mass spectrometry: application to a model bacterial biofilm. Environ Microbiol. 2000;2:530–541. doi:10.1046/j.1462-2920.2000.00136.x.
38. Jung C, Meinzer U, Montcuquet N, Thachil E, Chateau D, Thiebaut R, Roy M, Alnabhani Z, Berrebi D, Dussaillant M, et al. Yersinia pseudotuberculosis disrupts intestinal barrier integrity through hematopoietic TLR-2 signaling. J Clin Invest. 2012;122(6):2239–2251. doi:10.1172/JCI58147.
39. Bankhead P, Loughrey MB, Fernandez JA, Dombrowski Y, McArt DG, Dunne PD, McQuaid S, Gray RT, Murray LJ, Coleman HG, et al. QuPath: open source software for digital pathology image analysis. Sci Rep. 2017;7(1):16878. doi:10.1038/s41598-017-17204-5.
40. Schneider CA, Rasband WS, Eliceiri KW. NIH Image to ImageJ: 25 years of image analysis. Nat Methods. 2012;9:671–675. doi:10.1038/nmeth.2089.
41. Su L, Nalle SC, Shen L, Turner ES, Singh G, Breskin LA, Khramtsova EA, Khramtsova G, Tsai P, Fu Y, et al. TNFR2 activates MLCK-dependent tight junction dysregulation to cause apoptosis-mediated barrier loss and experimental colitis. Gastroenterology. 2013;145(2):407–415. doi:10.1053/j.gastro.2013.04.011.
42. Clayburgh DR, Barrett TA, Tang Y, Meddings JB, Van Eldik LJ, Watterson DM, Clarke, LL, Mrsny, RJ, Turner, JR. Epithelial myosin light chain kinase-dependent barrier dysfunction mediates T cell activation-induced diarrhea in vivo. J Clin Invest. 2005;115:2702–2715. doi:10.1172/JCI24970.
43. Marchiando AM, Shen L, Graham WV, Weber CR, Schwarz BT, Austin JR 2nd, Raleigh DR, Guan Y, Watson AJM, Montrose MH, et al. Caveolin-1-dependent occludin endocytosis is required for TNF-induced tight junction regulation in vivo. J Cell Biol. 2010;189:111–126. doi:10.1083/jcb.200902153.
44. Utech M, Ivanov AI, Samarin SN, Bruewer M, Turner JR, Mrsny RJ, Parkos, CA, Nusrat, A. Mechanism of IFN-gamma-induced endocytosis of tight junction proteins: myosin II-dependent vacuolarization of the apical plasma membrane. Mol Biol Cell. 2005;16:5040–5052.
45. Van Itallie CM, Fanning AS, Holmes J, Anderson JM. Occludin is required for cytokine-induced regulation of tight junction barriers. J Cell Sci. 2010;123:2844–2852. doi:10.1242/jcs.065581.
46. Foot N, Henshall T, Kumar S. Ubiquitination and the Regulation of Membrane Proteins. Physiol Rev. 2017;97:253–281. doi:10.1152/physrev.00012.2016.

47. Tanno H, Komada M. The ubiquitin code and its decoding machinery in the endocytic pathway. J Biochem. 2013;153:497–504. doi:10.1093/jb/mvt028.
48. Jennek S, Mittag S, Reiche J, Westphal JK, Seelk S, Dorfel MJ, Pfirrmann T, Friedrich K, Schütz A, Heinemann U, et al. Tricellulin is a target of the ubiquitin ligase Itch. Ann N Y Acad Sci. 2017;1397 (1):157–168. doi:10.1111/nyas.13349.
49. Traweger A, Fang D, Liu YC, Stelzhammer W, Krizbai IA, Fresser F, Bauer H-C, Bauer H. The tight junction-specific protein occludin is a functional target of the E3 ubiquitin-protein ligase itch. J Biol Chem. 2002;277:10201–10208. doi:10.1074/jbc.M111384200.
50. Piper RC, Dikic I, Lukacs GL. Ubiquitin-dependent sorting in endocytosis. Cold Spring Harb Perspect Biol. 2014;6:a016808. doi: 10.1101/cshperspect.a016808.
51. Tateda K, Ishii Y, Horikawa M, Matsumoto T, Miyairi S, Pechere JC, Standiford TJ, Ishiguro M, Yamaguchi K. The Pseudomonas aeruginosa autoinducer N-3-oxododecanoyl homoserine lactone accelerates apoptosis in macrophages and neutrophils. Infect Immun. 2003;71:5785–5793. doi:10.1128/IAI.71.10.5785-5793.2003.
52. Tao S, Luo Y, Bin H, Liu J, Qian X, Ni Y, Zhao R. Paraoxonase 2 modulates a proapoptotic function in LS174T cells in response to quorum sensing molecule N-(3-oxododecanoyl)-L-homoserine lactone. Sci Rep. 2016;6:28778. doi:10.1038/srep28778.
53. Odenwald MA, Turner JR. The intestinal epithelial barrier: a therapeutic target? Nat Rev Gastroenterol Hepatol. 2017;14:9–21.
54. Taguchi R, Tanaka S, Joe GH, Maseda H, Nomura N, Ohnishi J, Ishizuka, S, Shimizu, H, Miyazaki, H. Mucin 3 is involved in intestinal epithelial cell apoptosis via N-(3-oxododecanoyl)-L-homoserine lactone-induced suppression of Akt phosphorylation. Am J Physiol Cell Physiol. 2014;307:C162–8. doi:10.1152/ajpcell.00271.2013.
55. Neely AM, Zhao G, Schwarzer C, Stivers NS, Whitt AG, Meng S, Burlison, JA, Machen, TE, Li, C. N-(3-Oxoacyl)-homoserine lactone induces apoptosis primarily through a mitochondrial pathway in fibroblasts. Cell Microbiol. 2018;20:e12787.doi: 10.1111/cmi.12787.
56. Buschmann MM, Shen L, Rajapakse H, Raleigh DR, Wang Y, Wang Y, Lingaraju A, Zha J, Abbott E, McAuley EM, et al. Occludin OCEL-domain interactions are required for maintenance and regulation of the tight junction barrier to macromolecular flux. Mol Biol Cell. 2013;24(19):3056–3068. doi:10.1091/mbc.e12-09-0688.
57. Elias BC, Suzuki T, Seth A, Giorgianni F, Kale G, Shen L, Turner JR, Naren A, Desiderio DM, Rao R, et al. Phosphorylation of Tyr-398 and Tyr-402 in occludin prevents its interaction with ZO-1 and destabilizes its assembly at the tight junctions. J Biol Chem. 2009;284(3):1559–1569. doi:10.1074/jbc.M804783200.
58. Stamatovic SM, Johnson AM, Sladojevic N, Keep RF, Andjelkovic AV. Endocytosis of tight junction proteins and the regulation of degradation and recycling. Ann N Y Acad Sci. 2017;1397(1):54–65. doi:10.1111/nyas.13346.
59. Dorfel MJ, Huber O. Modulation of tight junction structure and function by kinases and phosphatases targeting occludin. J Biomed Biotechnol. 2012;2012:807356. doi:10.1155/2012/807356.
60. Murakami T, Felinski EA, Antonetti DA. Occludin phosphorylation and ubiquitination regulate tight junction trafficking and vascular endothelial growth factor-induced permeability. J Biol Chem. 2009;284:21036–21046. doi:10.1074/jbc.M109.016766.
61. Karlsson T, Turkina Mv F, Yakymenko O, Yakymenko O F, Magnusson K-E, Magnusson Ke F, Vikstrom E, Vikstrom E. The Pseudomonas aeruginosa N-acylhomoserine lactone quorum sensing molecules target IQGAP1 and modulate epithelial cell migration. PLoS Pathog. 2012. doi:10.1371/journal.ppat.1002953.
62. Jahoor A, Patel R, Bryan A, Do C, Krier J, Watters C, Wahli W, Li G, Williams SC, Rumbaugh KP, et al. Peroxisome proliferator-activated receptors mediate host cell proinflammatory responses to pseudomonas aeruginosa autoinducer. J Bacteriol. 2008;190 (13):4408–4415. doi:10.1128/JB.01444-07.
63. Maurer S, Wabnitz GH, Kahle NA, Stegmaier S, Prior B, Giese T, Gaida MM, Samstag Y, Hänsch GM. Tasting pseudomonas aeruginosa biofilms: human neutrophils express the bitter receptor T2R38 as sensor for the quorum sensing molecule N-(3-Oxododecanoyl)-l-homoserine lactone. Front Immunol. 2015;6:369. doi:10.3389/fimmu.2015.00369.